Am J Cancer Res 2021;11(3):930-944
www.ajcr.us /ISSN:2156-6976/ajcr0127943

Original Article

Loss of BRMS2 induces cell growth inhibition and translation capacity reduction in colorectal cancer cells

Yaofu Liu[1], Weimin Xu[2], Xin Xu[1], Zhengzhi Tan[3], Jing Xu[4], Lei Ma[1], Peng Du[2], Yili Yang[1,5]

[1]*Suzhou Institute of Systems Medicine, Chinese Academy of Medical Sciences & Peking Union Medical College, Suzhou, China;* [2]*Department of Colorectal Surgery, Xin-Hua Hospital, Shanghai Jiaotong University School of Medicine, Shanghai, China;* [3]*Department of Computer Science, University of Alabama at Birmingham, Birmingham, USA;* [4]*International School for Advanced Studies (SISSA), Trieste, Italy;* [5]*China Regional Research Center, International Centre for Genetic Engineering and Biotechnology, Taizhou, Jiangsu, China*

Received December 9, 2020; Accepted January 12, 2021; Epub March 1, 2021; Published March 15, 2021

Abstract: A variety of chemotherapeutic drugs targeting ribosome processing have been developed and applied to cancer treatment mainly based on the impaired ribosome biogenesis checkpoint (IRBC). The IMP U3 small nucleolar ribonucleoprotein 3 (IMP3, BRMS2) has been identified as a participant in pre-rRNA processing for nearly twenty years. However, the roles of BRMS2 in cancers still unknown. In this research, a tissue microarray (TMA) with 151 paired tissues showed the aberrant overexpression of BRMS2 in CRC tissues which was associated with the worse prognosis. To clarify the function of BRMS2 in CRC cells, an inducible knockdown system was introduced *in vitro* and *in vivo* and the cell growth was drastically suppressed. Mechanistically, we found depletion of BRMS2 markedly decreased the protein translation rates which can limit cell growth. Furthermore, to confirm whether the IRBC played a role, multiple approaches including detection of the p53 pathway, depletion of BRMS2 in p53-mutated SW620 cells, and co-depletion of RPL11 were taken. To our surprise, IRBC was not activated. That indicated BRMS2 may play a unique role in ribosome biosynthesis and IRBC. Taken together, our results demonstrated the oncogenic function of BRMS2 in CRC cells and supported its potential as a therapeutic target.

Keywords: IMP U3 small nucleolar ribonucleoprotein 3, colorectal cancer, cell growth, protein translation, impaired ribosome biogenesis checkpoint

Introduction

Ribosomes are found in all living cells which are essential for protein production and thus for cell growth and proliferation. Ribosome biogenesis is an elaborate and well-coordinated process which is regulated by numerous pathways. Several studies have demonstrated that the disruption of ribosome biogenesis at various steps could result in cell cycle arrest mainly through the RPL5/RPL11/5S rRNA/Hdm2/p53 axis [1]. Under normal conditions, p53 is continuously expressed but kept at a low level. Its low level is maintained mainly through an E3 ubiquitin ligase, Hdm2. It has been reported that Hdm2 can ubiquitylate p53 and stimulate the nuclear export of p53 for proteasome-mediated degradation [2]. Disruption of ribosomal biogenesis led to the spontaneous release of ribosome components including ribosome proteins (RPs) and rRNA into the nucleoplasm. These components could bind to the central acidic domain of Hdm2 and blocked its p53 ubiquitination and degradation function, resulting in activation of p53 and cell cycle arrest [3]. This particular process was termed as the impaired ribosome biogenesis checkpoint (IRBC) [4]. The maturation of rRNA is one of the most important steps. Depletion, mutation or overexpression of rRNA maturation-associated factors have been shown to induce IRBC [5].

BRMS2 is a component of U3 small nucleolar ribonucleoprotein complex (U3 snoRNP), a subset of box C/D snoRNPs [6]. U3 snoRNP functions in rRNA maturation by directing pre-rRNA cleavage. Conditional repression of U3 synthesis could inhibit cleavage in the 5'ETS of yeast pre-rRNA and impaired formation of 18S rRNA.

These progresses were accompanied by progressively decreased growth [7]. During this process, BRMS2, together with IMP4 and MPP10, might function by facilitating or stabilizing base-pairing interactions between U3 snoRNA and the pre-rRNA [8]. As a result, BRMS2 may play roles in cell growth. However, the relationship between BRMS2 and cancers remains unknown.

Colorectal cancer (CRC) is the third (10.2%) most commonly diagnosed and second mortal (9.2%) cancer [9]. More than 1.8 million new colorectal cancer cases with almost 900,000 deaths annually [10]. The prognosis of CRC is far from satisfied even though the advance of comprehensive treatment strategies including surgery, chemotherapy, and radiotherapy over the past few decades. Therefore, it is meaningful to explore novel molecule mechanisms to be as effective therapeutic targets in clinical practice. We are wondering whether BRMS2 could potentially serve as a new therapeutic target for CRC.

In this research, we first found BRMS2 was aberrantly over-expressed in CRC tissues and it was an adverse prognostic factor correlated with a series of clinicopathologic characteristics. Additionally, knockdown of BRMS2 induced inhibition of cell growth both *in vitro* and *in vivo* without activation of IRBC but was accompanied by reduced translation capacity. Thus, our data provided a link between BRMS2 and CRC development and indicated that targeting BRMS2 may be an effective strategy to inhibit CRC.

Materials and methods

Patients and immunohistochemical analysis

The patients' information and baseline characteristics have been described in the previous study [11]. Cancer and its para-cancerous normal mucosa embedded with paraffin were made into TMA for further immunohistochemistry (IHC) analysis. The staining of TMA and xenograft tumor sections were conducted by using the IHC kit (G1215, Servicebio, Wuhan, China) according to the manufacturer's protocol. The results of immunostaining were determined by immunoreactive score (IRS): IRS = SI (staining intensity) × PP (percentage of positive cells). SI was determined as: negative = 0, weak = 1, moderate = 2, strong = 3; Staining intensity: negative = 0, weak = 1, moderate = 2, strong = 3; additionally, the PP was defined as: negative = 0, 1~10% = 1, 11~50% = 2, 51~80% = 3, 80~100% = 4 [12]. Immunohistochemical scores were independently determined by two pathologists. Twelve pairs of tissues were confirmed by western blots. The use of human tissues in this study was authorized by the Ethics Committee of Xinhua Hospital and informed consents were obtained for all the collections.

Cell culture and reagents

CRC cell lines HCT116, Lovo and SW620 were purchased from American Type Culture Collection, Maryland, USA. HEK293T cell line was kindly provided by Dr. Kunkun Han from The Asclepius Technology Company Group and Asclepius Cancer Research Center, Suzhou, Jiangsu, China. These cells were cultured in Dulbecco's modified Eagle's medium (DMEM) supplemented with 10% fetal bovine serum (FBS; Gibco, New York, USA) and incubated at 37°C with 5% CO_2. The p53 sequence of those three CRC cell lines were verified by Sanger sequencing.

Plasmid construction, lentivirus production, and infection

The annealed shNC, shBRMS2, and shRPL11 sequences were introduced into Tet-pLKO-puro vector (Addgene, #21915) or Tet-pLKO-neo (Addgene, #21916) by using AgeI and EcoRI restriction sites. Three gene-specific shRNAs targeting BRMS2 or RPL11 were designed and the highest efficiency one was used in further investigation. The sequences of these shRNAs were shown in Table S1. For lentiviral packaging, each of the recombinant vectors was co-transfected with the psPAX2 lentivirus-packaging vector and the PMD2G lentivirus-envelope plasmid (Gifts from Dr. Xiaodan Hou, Suzhou Institute of Systems Medicine, Suzhou, Jiangsu, China) in HEK293T cells by using polyethylenimine (Sigma-Aldrich, Missouri, USA) according to the manufacturer's instructions. Lentivirus particles were infected into the CRC cells in the presence of 6 μg/ml polybrene. Stable cell lines were further selected with 0.6 μg/ml puromycin (Sigma-Aldrich, Missouri, USA) or 700 μg/ml G418 (BBI-lifesciences, Shanghai, China) for 2 weeks. CRC cells were treated with 1 μg/ml doxycycline hyclate (Dox, Sigma-Aldrich, Missouri, USA) for inducing the shRNAs [13].

RNA isolation and qRT-PCR

Total RNA was extracted using RNAiso Plus Reagent (Takara, Dalian, China). An amount of 1 μg total RNA was then reverse-transcribed into cDNA using the PrimeScriptTM RT reagent Kit with gDNA Eraser (Takara, Dalian, China) according to the manufacturer's instructions. The qRT-PCR was carried out using SYBR Green qPCR Master Mix (Takara, Dalian, China) and Applied Biosystems 7500 Fast Real-Time PCR System (Applied Biosystems, Waltham, USA). Expression data were normalized to the mRNA levels of the GAPDH housekeeping gene and calculated using the $2^{-\Delta\Delta Ct}$ method. The primer sequences are shown in Table S1. Of note, pre-47s primer sequences were referred from previous study [14].

RNA sequencing and bioinformatics analysis

Total RNA of NC-KD and BRMS2-KD HCT116 cells exposed to Dox was extracted using RNAiso Plus Reagent and sequenced by Genewiz (Suzhou, China). Raw data was analyzed using the CLC Genomics Workbench (Qiagen, Aarhus, Demark). Human genome reference sequence hg38 (NCBI) and 1000 Genomes Project (Phase 3, Ensembl version 91) were employed for mapping. The expression value of RNAseq was expressed as Transcripts Per Kilobase of exon model per Million mapped reads (TPM). The fold change between the two groups was Logged and used for draw heatmap. The Heatmap was generated using ComplexHeatmap package writing on R studio.

Western blot (WB) analysis

Protein extracts were isolated using RIPA lysis buffer supplemented with protease inhibitor cocktail (MCE, New Jersey, USA) and protein concentration was measured with BCA Protein Assay Reagent (Beyotime, Beijing, China). 30~50 μg protein was separated by SDS-PAGE gels and transferred to PVDF membranes (Sigma-Aldrich, Missouri, USA). The membranes were blocked with 5% non-fat milk for 1 h at room temperature (RT) and then incubated with primary antibodies at 4°C overnight. The antibodies used in this study were as follows: BRMS2 (CSB-PA290241, CUSABIO, Wuhan, China), RPL11 (ab264342, Abcam, Cambridge, UK), GAPDH (60004-1-Ig, Proteintech, Wuhan, China), PARP (9532, Cell Signaling, Danvers, USA), Cyclin D1 (A5035, Bimake, Houston, USA), p53 (60283-2-Ig, Proteintech, Wuhan, China), and p21 (2947, Cell Signaling, Danvers, USA). Bands were analyzed by enhanced chemiluminescence system (BioRad, California, USA) with GAPDH as a loading control.

Cell counting kit-8 (CCK8)

To assess the effect of BRMS2 knockdown on the cell proliferation ability, 1500/well NC-KD or BRMS2-KD CRC cells were seeded into 96-well plates, and incubated with or without 1 μg/μl Dox in 200 μl complete medium. After incubation for 24 h, each well was added with 20 μl CCK-8 solution and incubated for 1 h at 37°C. The plates were read by a microplate reader at 450 nm for consecutive 6~7 days. The medium was refreshed every 72 h.

Flow cytometry for cell cycle and apoptosis

NC-KD or BRMS2-KD HCT116 cells exposed to Dox or not were digested by trypsin and washed twice with cold PBS, then fixed by 70% ice-cold ethanol at -20°C overnight. Cells were stained with 0.5 ml Propidium Iodide (PI)/RNase staining buffer (550825, BD Pharmingen, San Diego, USA) for 15 min at RT and analyzed by flow cytometry (Thermo Fisher scientific, Waltham, USA). To detect the cells undergoing apoptosis, those cells were stained with Annexin V and PI (556547, BD Pharmingen, New Jersey, USA) according to the manufacturer's instructions. Briefly, cells were washed twice with cold PBS and then resuspended in 1 × Binding Buffer at a concentration of 1×10^5 cells/100 μl. 5 μl FITC-Annexin V and 5 μl PI were added. The cells were gently mixed and incubated for 15 min at RT in the dark. Finally, 400 μl 1 × Binding Buffer was added into each tube and flow cytometry was preformed within 1 h. The results of flow cytometry were analyzed by FlowJo (Version 10).

Tumor xenografts in nude mice

The animal study was approved by the Review Board of Animal Care and Use of Suzhou Institute of Systems Medicine. A total of 1×10^7 BRMS2-KD or NC-KD HCT116 cells were suspended in 100 μl serum-free DMEM medium and inoculated subcutaneously in the flank of 8-week-old male BALB/C Nude mice (n = 16, 8/group). The mice were put on Dox-containing

chow (625 mg/kg, BiotechHD, Beijing, China) 3 days before implantation [15]. Throughout the experiment, tumor volumes were monitored every day after implantation. At the end of the experiment, mice were euthanized and tumors were excised, weighted, and subjected to other experiments.

Translation assay

To quantify the protein translation rate after BRMS2 depletion, we used the non-radioactive metabolic labelling assay kit "Click-iT HPG Alexa Fluor 488 Protein Synthesis Assay Kit" (C10428, Thermo Fisher Scientific, Waltham, USA) to measure the global translation according to the manufacturer's protocol. Briefly, cells were pre-cultured in L-methionine-free medium for 45 min to deplete endogenous methionine. 50 μM HPG was added to the culture medium and incubated for 30 min. Then, cells were fixed in situ or digested by trypsin and undergo next steps in the tube. After fixation, 0.5% Triton X-100 in PBS was added and incubated for 20 min at RT. The azide-alkyne cycloaddition was performed using the Alexa Fluor 488 azide and incubated for 30 min at RT, protected from light. After DNA staining using HCS NuclearMask Blue, the cells were recorded by fluorescence microscopy (Nikon) or flow cytometry [16]. The mean fluorescence intensities were analyzed by Image J and normalized by the mean fluorescence intensity of the NC-KD HCT116 cells.

Statistical analysis

GraphPad Prism 8 and SPSS 13.0 were used for statistical analyses. Quantitative variables were analyzed by Student's *t* test. The relationships between BRMS2 expression and clinicopathologic variables were analyzed using the Chi-square and Fisher's exact tests. Kaplan-Meier survival curves were constructed, and the log-rank test was performed to assess patients' survival. $P<0.05$ was considered statistically significant for all analyses.

Results

Aberrant overexpression of BRMS2 in colorectal cancer patients is associated with worse prognosis

To investigate the role of BRMS2 in CRC cells, we firstly evaluated the expression of BRMS2 in 12-paired normal and CRC tissues by western blot. As shown in **Figure 1A** and **1B**, BRMS2 protein levels were significantly increased in CRC tumor tissues compared with the paired normal paracancerous tissues. Furthermore, this result was confirmed by IHC staining in a TMA with 151 CRC tumor tissues and paired normal colon tissues. Representative BRMS2 IHC staining images were presented in **Figure 1C**. Among the 151 patients, percentage of BRMS2-high expression in CRC tissues (45.70%) was higher than that in normal tissues (9.93%) (**Figure 1D**; **Table 1**).

Based on IHC staining of CRC tissues, all patients were divided into a low-BRMS2 group (IRS scrore ≤8, N = 82) and a high-BRMS2 group (IRS scrore >8, N = 69). The relationship between BRMS2 expression and the prognosis was evaluated then. In the Kaplan-Meier survival analysis, overall survival (OS) ($P<0.0001$) and disease-free survival (DFS) ($P<0.0001$) in the low-BRMS2 group were significantly better than those in the high-BRMS2 group (**Figure 1E**, **1F**).

Clinicopathologic significance of BRMS2 expression in CRC patients

To explore whether BRMS2 was associated with the clinical characteristics of CRC patients, we compared several clinical and pathologic factors (**Table 1**) of the 151 patients. No significant difference was observed in gender ($P = 0.534$), age ($P = 0.974$), location ($P = 0.769$) and CEA level ($P = 0.602$) between the low-BRMS2 group and the high-BRMS2 group. However, a significant difference was found in extent of invasion ($P = 0.010$), lymphatic metastasis ($P = 0.022$), metastasis ($P = 0.033$) and TNM stage ($P = 0.016$).

Loss of BRMS2 attenuates the proliferation of CRC cells by blocking cell-cycle instead of inducing cell apoptosis in vitro

Given that high BRMS2 was associated with worse prognosis, we then investigated the biological function of BRMS2 in CRC cells. As shown in **Figure 2A**, the protein expression of BRMS2 was detected in 6 CRC cell lines and it was highly expressed in HCT116 cells while lowly expressed in LoVo cells.

To further evaluate the role of BRMS2 in cell growth, we introduced a Dox-inducible shRNA to knock down BRMS2 both in HCT116 and

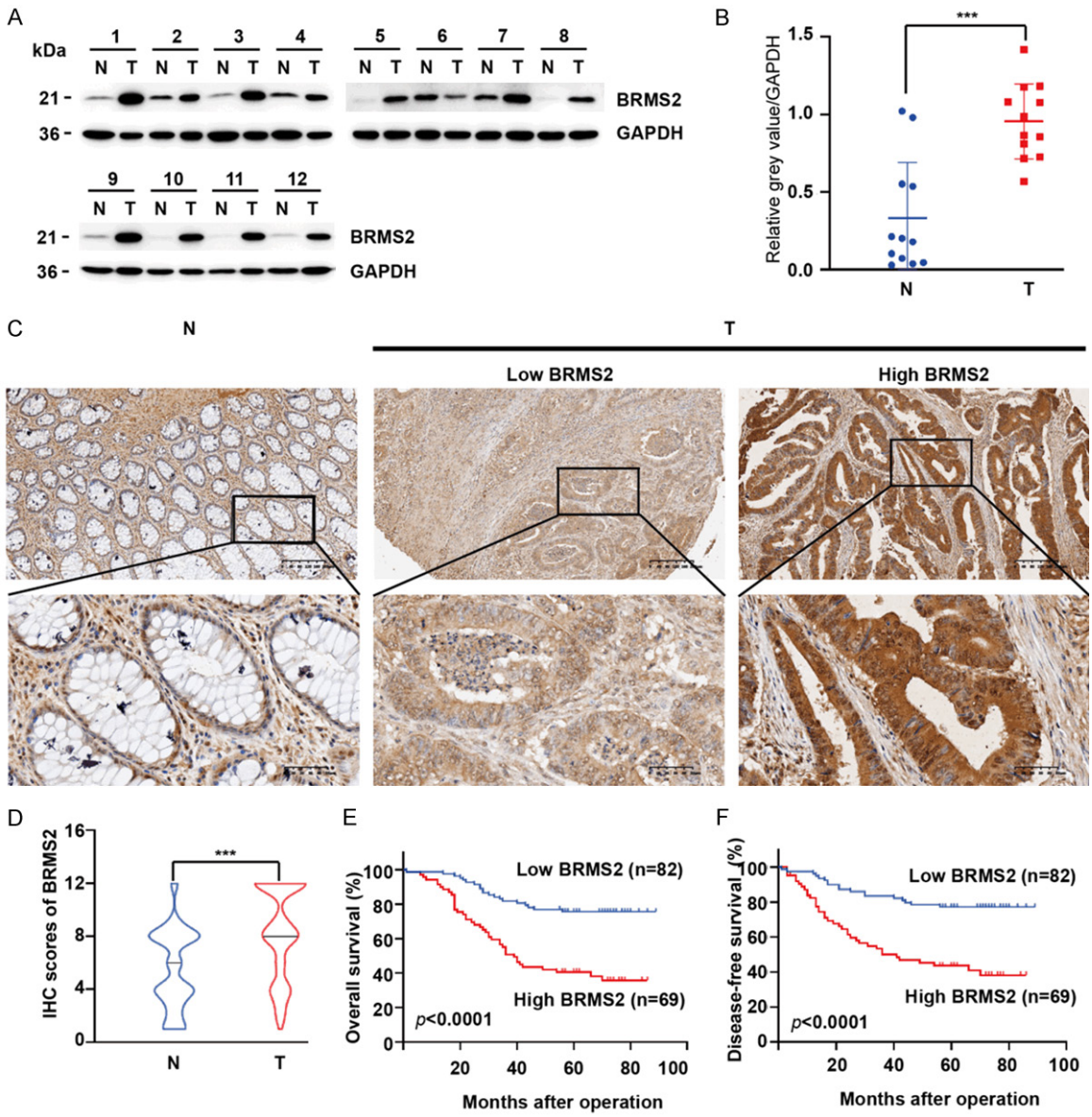

Figure 1. Increased BRMS2 expression in CRC tissues predicts worse prognosis. (A, B) BRMS2 expression in 12 paired CRC samples were detected by western blot (A), and relative grey values of bands were quantified (B). (C) The representative immunohistochemical images of paracancerous normal tissues and tumor tissues in tissue microarray (magnification: × 100, upper panels; × 400, lower panels). (D) The violin plot of tissue microarray indicated IHC scores of tumor tissues was significantly higher than normal tissues. (E, F) The Kaplan-Meier plots were stratified by BRMS2 expression for overall survival (E) and disease-free survival (F) in CRC patients. N: normal tissues; T: tumor tissues. $^{*}P<0.05$, $^{**}P<0.01$, $^{***}P<0.001$.

LoVo cells using a lentivirus-mediated system. Dox was added to induce BRMS2 knockdown and the efficiency was confirmed by qRT-PCR (**Figure 2B**) and western blot (**Figure 2F**). As the outcome of BRMS2 knockdown, pre-47S RNA was accumulated (**Figure 2C**).

Next, to examine whether BRMS2 silence inhibited CRC proliferation, CCK-8 assay was carried out to measure cell viability in the two cell lines. As shown in **Figure 2D**, **2E**, BRMS2-KD HCT116 or LoVo cells exposed to Dox exhibited significant loss of viability in contrast to the control cells or the BRMS2-KD cells without supplying with Dox. Moreover, the proliferation-inhibition effect of HCT116 was stronger than that in LoVo following BRMS2 knockdown.

Those results demonstrated a link between BRMS2 expression and CRC cell growth. There-

Table 1. Relationship between BRMS2 expression and clinicopathologic variables in 151 CRC patients

Characteristic	Case (151)	BRMS2 expression		X^2 value	P
		Low	High		
Tissues				48.090	0.000
N	151	136	15		
T	151	82	69		
Gender				0.386	0.534
Male	79	41	38		
Female	72	41	31		
Age				0.001	0.974
<65 y	72	39	33		
≥65 y	79	43	36		
Location				0.525	0.769
Left hemicolon	53	28	25		
Right hemicolon	30	15	15		
Rectum	68	39	29		
Extent of invasion				11.286	0.010
T1	2	2	0		
T2	12	8	4		
T3	42	30	12		
T4	95	42	53		
Lymphatic metastasis				7.652	0.022
N0	71	47	24		
N1	52	23	29		
N2	28	12	16		
Metastasis				4.524	0.033
M0	132	76	56		
M1	19	6	13		
TNM stage				10.305	0.016
I	12	8	4		
II	54	36	18		
III	69	34	35		
IV	16	4	12		
CEA level				0.272	0.602
<10 ng/ml	104	55	49		
≥10 ng/ml	47	27	20		

fore, we next sought to uncover the causes of loss of viability when BRMS2 depletion. As a result, cell cycle and apoptosis in HCT116 cells were investigated using western blot. We found Cyclin D1 was notably decreased when BRMS2-KD cells were exposed to Dox, while reduction of BRMS2 expression did not influence the cleaved-PARP level (**Figure 2F**). To validate this observation, flow cytometry was performed to detect cell cycle and apoptosis. Consistent with above findings, cell cycle analysis revealed that BRMS2-conditional depletion increased the percentage of cells in G1 phase (P<0.0001) (**Figure 2G**, **2H**). Moreover, no significant change was observed in apoptosis analysis (**Figure 2I**, **2J**).

Conditional depletion of BRMS2 does not induce p53 stabilization

BRMS2 has been identified as a participator in pre-18S rRNA processing [8], as a result, it was not weird for BRMS2 depletion to active p53 pathway and induce IRBC. To address this hypothesis, we first detected the protein levels of p53 and p21 in NC-KD and BRMS2-KD HCT116 cells exposed to Dox for 0 d, 3 d or 5 d. Intriguingly, protein level of p53 was slightly down-regulated instead of up-regulated as the expectation when BRMS2 was conditionally depleted. This result was supported by p21 in western blot which was significantly decreased too (**Figure 3A**). In NGS analysis, most of p53 target genes listed by KEGG (map04115) were downregulated (**Figure 3B**).

Treating BRMS2-KD HCT116 cells with Dox for 0 h to 72 h, we found the inhibition of p53 pathway was a time-dependent process and p53 was never activated during this process (**Figure 3C-F**). BRMS2 mRNA was significantly down-regulated when BRMS2-KD HCT116 cells exposed to Dox for 6 h and decreased further until about 24 h (**Figure 3C**). pre-47s was accumulated depending on the depletion of BRMS2 (**Figure 3D**). p21 and GADD45G which were down-regulated in the NGS analysis, were taken as represent target genes of p53. As expectation, p21 and GADD45G were significantly down-regulated depending on BRMS2 depletion (**Figure 3E**, **3F**). These results indicated p53 might not be activated when BRMS2 was depleted.

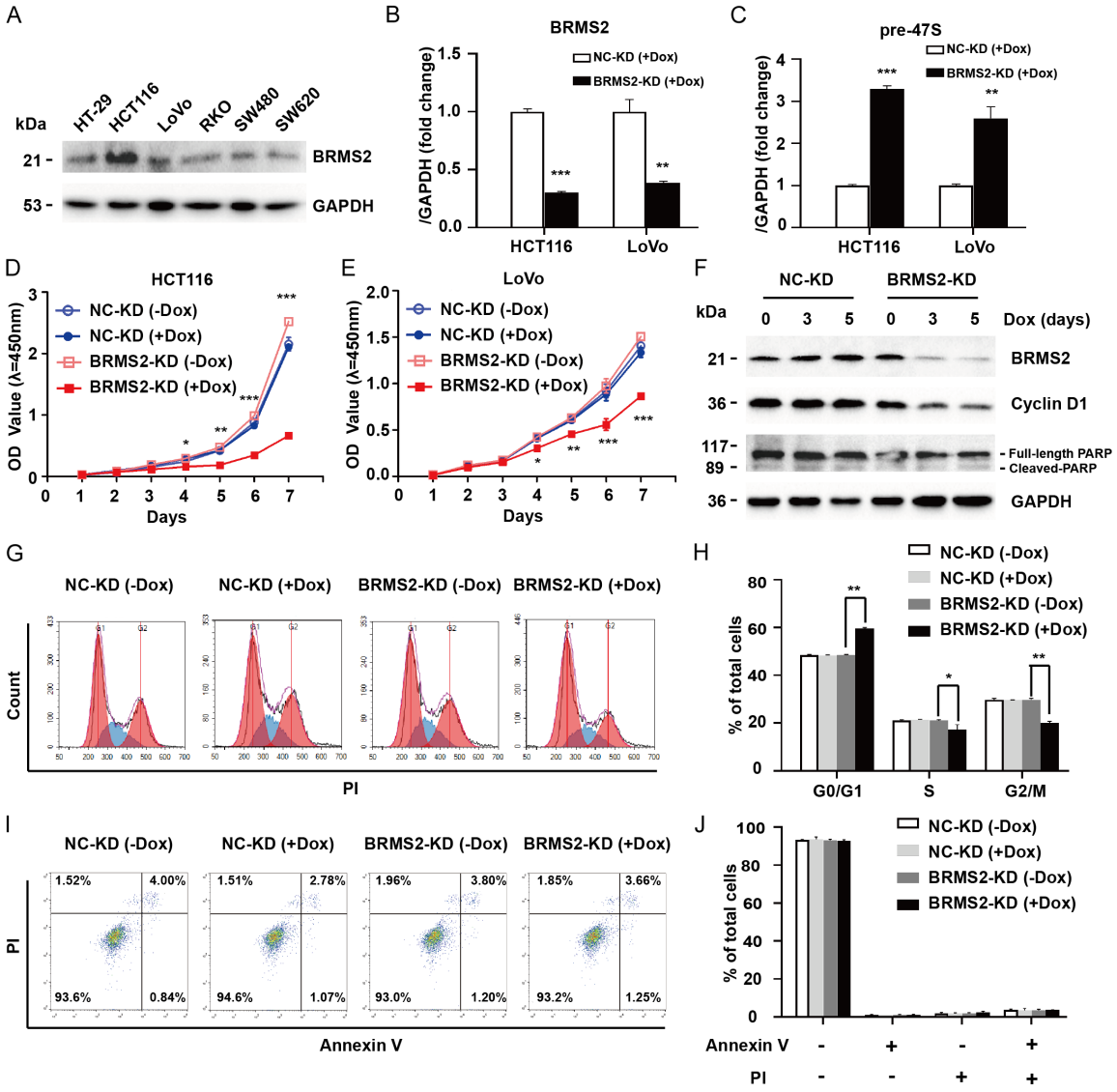

Figure 2. Loss of BRMS2 impedes proliferation in CRC cells by inducing cell cycle block rather than cell apoptosis. A. BRMS2 expression in six CRC cell lines detected by western blot. B, C. QPCR analysis of BRMS2 and pre-47S expression level in HCT116 and LoVo cells transduced with NC and BRMS2 shRNA TET-ON virus in the presence of Dox. GAPDH served as an internal control. D, E. The proliferation of BRMS2-knockdown HCT116 and LoVo cells in the absence and presence of Dox was analyzed by CCK-8 assay. The cell numbers were analyzed every day for 7 days. F. Western blot was performed to detect BRMS2, Cyclin D1, and PARP expression after cells were induced by Dox for 0, 3, and 5 days. GADPH served as an internal control. G, H. Flow cytometry was performed to detect cell cycle after cells were induced by Dox in NC-KD and BRMS2-KD HCT116 cells. I, J. No significant change of cell apoptosis was observed when analyzed by flow cytometry in Dox induced BRMS2-knockdown HCT116 cells. $^{*}P<0.05$, $^{**}P<0.01$, $^{***}P<0.001$.

To further confirm whether p53 played a role in BRMS2 depletion-induced proliferation inhibition, we knocked down BRMS2 in SW620 cells whose p53 was mutated. Consistent with results in HCT116 cells, cell proliferation was slowed down when BRMS2-KD SW620 cells exposed to Dox (**Figure 3G-I**). Cyclin D1, p21, and p53 were also lowly expressed (**Figure 3H**).

Another approach we took was co-inhibiting RPL11 and BRMS2 at the same time in HCT-116 cells. Previously studies indicated RPL11 could be over-expressed in face of several ribosome biogenesis stress factors and knockdown of RPL11 led to the abrogation of p53 stabilization [17]. If the IRBC existed in the BRMS2-knockdown cells, further knocking do-

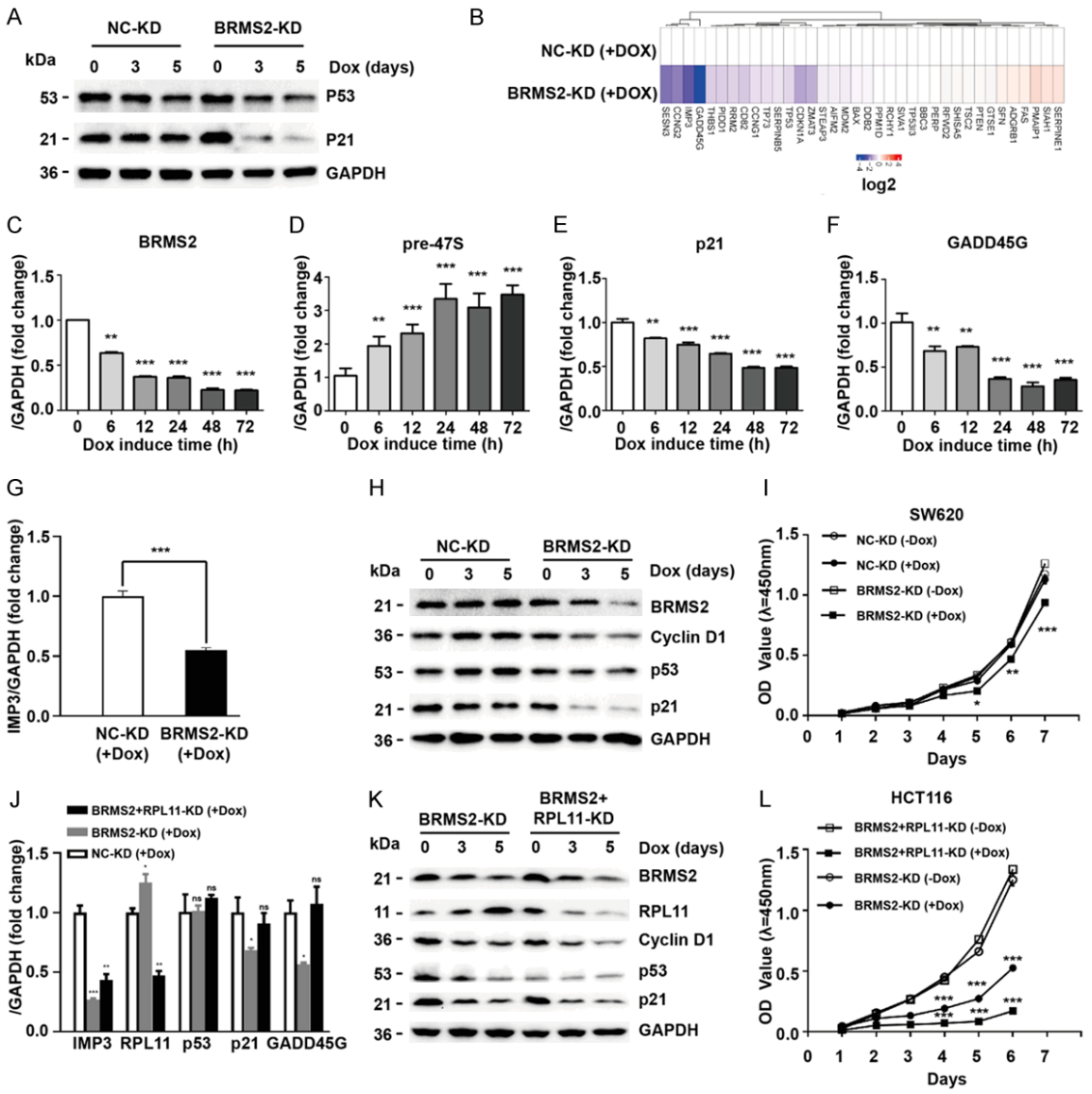

Figure 3. Cell cycle block after BRMS2 knockdown is not result from ribosome biogenesis stress. A. Western was performed to detect p53 and p21 expression after Dox induced NC and BRMS2-knockdown HCT116 cells for 0, 3, and 5 days. GADPH served as an internal control. B. The expression of BRMS2 and downstream genes of p53 were detected by RNA-seq after Dox induced NC and BRMS2-knockdown HCT116 cells. The set of genes were collected from KEGG. Most downstream genes of p53 were down-regulated. C-F. QPCR analysis of BRMS2, pre-47S, p21, GADD45G expression level in HCT116 after Dox induced BRMS2 knockdown for 0, 6, 12, 24, 48 and 72 h. G. QPCR analysis of BRMS2 expression level after Dox induced NC and BRMS2-knockdown SW620 cells in which p53 was mutated. H. Western blot was performed to detect BRMS2, Cyclin D1, p53 and p21 expression after Dox induced NC and BRMS2-knockdown SW620 cells for 0, 3, and 5 days. I. The proliferation of BRMS2-knockdown SW620 cells in the absence and presence of Dox was analyzed by CCK-8 assay. The cell numbers were analyzed every day for 7 days. J. QPCR analysis of BRMS2, RPL11, p53, p21, and GADD45G expression level after Dox induced NC, BRMS2 depletion alone or BRMS2 and RPL11 co-depletion. K. Western blot was performed to detect BRMS2, RPL11, Cyclin D1, p53 and p21 expression after Dox induced BRMS2 depletion alone or BRMS2 and RPL11 co-depletion. L. CCK8 assay was used to analyze the proliferation of HCT116 cells with BRMS2 knockdown alone or BRMS2 and RPL11 knockdown together. The cell numbers were analyzed every day for 6 days. $^{*}P<0.05$, $^{**}P<0.01$, $^{***}P<0.001$.

wn RPL11 might rescue the proliferation-inhibition effects. As **Figure 3J**, **3K** shown, BRMS2 and RPL11 were knocked down at the same time in HCT116 cells when exposing to Dox. Additionally, RPL11 was over-expressed when BRMS2 was interfered as expectation, even though the up-regulated RPL11 did not act as the p53 stabilizer in BRMS2-KD cells (**Figure**

3J, **3K**). However, the proliferation inhibition was not relieved and even severer when RPL11 was knocked down (**Figure 3L**). Take together; our data indicated that p53 or IRBC may not play the central role in BRMS2-depletion-induced proliferation inhibition.

BRMS2 depletion impairs CRC tumor growth but not activate p53 signaling in nude mice

The effects of BRMS2 deficiency on CRC cell proliferation *in vitro* prompted us to examine whether BRMS2 depletion could inhibit CRC tumor growth *in vivo*. We injected Dox-inducible NC-KD or BRMS2-KD HCT116 cells into 8-week-old nude mice. Consistent with the effects *in vitro*, BRMS2-KD HCT116 xenograft tumors showed more than 50% inhibition in growth compared with the NC-KD tumors (**Figure 4A**). About 14 days after implantation, mice were sacrificed and tumors were excised for further measurement and detection. The excised tumors were aligned for comparison (**Figure 4B**). In agreement to the tumor volume, the weight of BRMS2-KD tumors was reduced about to 30% of the weight of NC-KD tumors (**Figure 4C**).

As shown in **Figure 4D-G**, the qRT-PCR, western blot, and IHC confirmed that inducible BRMS2 knockdown resulted in downregulation of BRMS2 mRNA and protein levels. The pre47s was accumulated as the outcome of BRMS2 depletion (**Figure 4D**). Consistent with the slowed growth, expression of Cyclin D1 was down-regulated in BRMS2-KD tumors. Additionally, p53 and p21 were also lowly expressed consistent with our *in vitro* data. Collectively, our findings indicated that BRMS2 knockdown significantly inhibited CRC cells growth *in vitro* and *in vivo*. Moreover, the effects were not dependent on activation of p53 or IRBC.

Translation rate is reduced when knocking down BRMS2

Previous studies have shown that loss of RPL5 and RPL11 impeded cell proliferation mainly due to the reduced translation capacity [18]. BRMS2 was reported to help mediate the U3 snoRNA-pre-rRNA base-pairing interactions which was important for ribosome biogenesis [19]. As a result, we reasoned that the inhibited proliferation of BRMS2 depletion might duo to the reduced protein translation. To address this, we measured the translation rate by L-HPG incorporation into nascent proteins. As shown in **Figure 5A**, **5B**, the translation rate in BRMS2-KD HCT116 cells was decreased more than half compared with the NC-KD cells. The signal intensity of nascent proteins measured by flow cytometry showed similar results (**Figure 5C**, **5D**). Those results indicated reduced translation capacity rather than activation of p53 played the main role in BRMS2 suppression-mediated growth inhibition.

Discussion

Nowadays, the functions of BRMS2 have not been comprehensively understood. The main known one is that BRMS2 was required for the early cleavages during pre-18S rRNA processing by mediating the formation of U3-pre-rRNA duplexes [8, 19, 20]. However, the role of BRMS2 in cancer development is largely unknown. In this study, we firstly uncovered the aberrant overexpression of BRMS2 in CRC cells and its biological function in promoting cell proliferation. This proposes that BRMS2 could be a putative therapeutic target for CRC. Moreover, the therapeutic effect of BRMS2 depletion is accompanied by reduced translation rate rather than IRBC.

It has been reported that ribosome is essential for protein translation, and thus for cell growth and proliferation [21]. Hyperactive ribosomal biogenesis is the main characteristic of cancers cells [22]. Ribosome biogenesis begins with transcription of rRNA by RNA polymerases I and it is the rate-limiting step in ribosome production [23]. Then, the maturation of rRNA is coordinated mainly by box C/D and box H/ACA snoRNPs. C/D snoRNPs components such as snoRNP proteins methyltransferase fibrillarin (FBL) or snoRNAs U3 and U8 have been shown to be upregulated in several cancer types [24, 25]. As a result, it is not wired for us to uncover the aberrant overexpression of BRMS2 in CRC cells. Moreover, our results showed that the high expression level of BRMS2 in tumor tissues was associated with worse prognosis.

Previous studies indicated increased activity of the ribosome biogenesis was not only required for the rapid proliferation of cancer cells, but might also serve as a driving force in malignancy [26]. As a result, ribosome biogenesis has

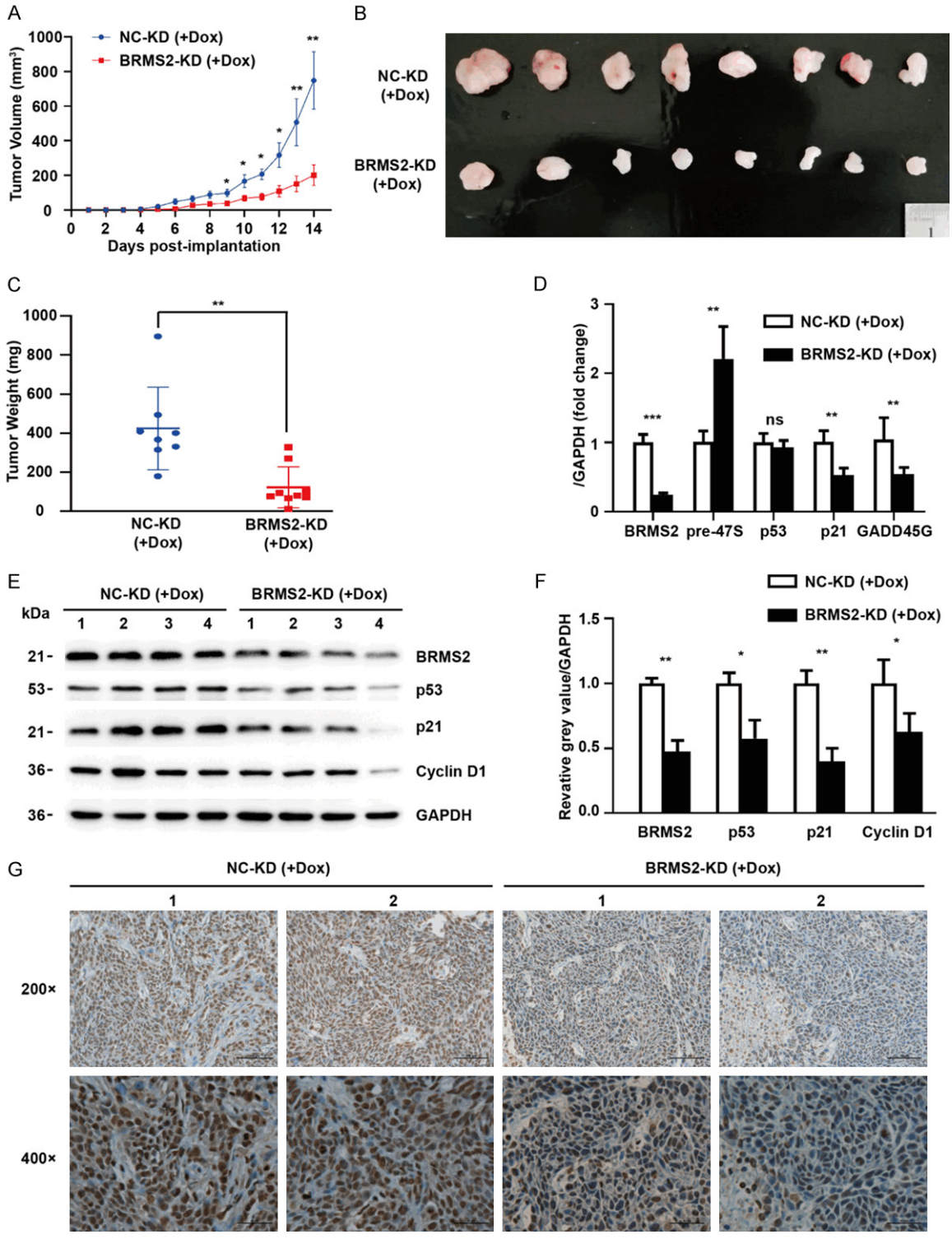

Figure 4. BRMS2 knockdown inhibits tumor growth in CRC in vivo. 10 million NC-KD or BRMS2-KD HCT116 cells were inoculated into mice to create a xenograft tumor model. Mice were randomized into two groups (8 mice/group). The mice were fed dox-containing chow (625 mg/kg) for 3 days with Dox prior to inoculation and after inoculation until sacrifice. A. The tumor volumes were recorded in both groups. B. Images of tumors were taken from both groups after 2 weeks of treatment. Tumors derived from the BRMS2-KD HCT116 cells were significantly smaller compared with the NC-KD group. C. The tumor weight were measured too. D. QPCR analysis of BRMS2, pre-47S, p53, p21, and GADD45G expression level in NC-KD or BRMS2-KD group in vivo. E, F. Western blot was performed to detect BRMS2, Cyclin D1, p53 and p21 expression in NC-KD or BRMS2-KD group in vivo and quantification of relative grey value of bands were compared with GAPDH. G. Immunohistochemical analysis of BRMS2 expression in tumors from the two groups (magnification: × 200, upper panels; × 400, lower panels). $^{*}P<0.05$, $^{**}P<0.01$, $^{***}P<0.001$.

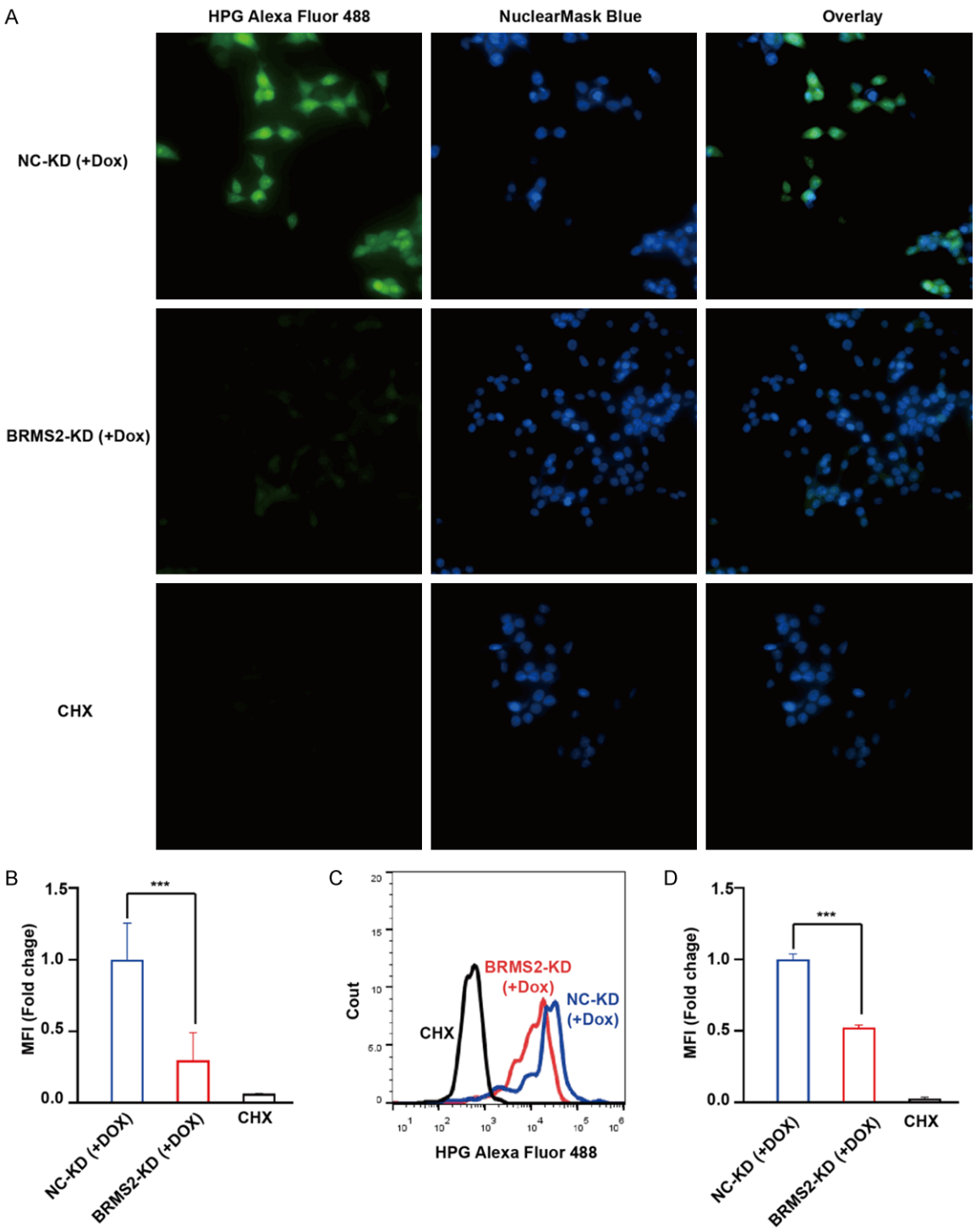

Figure 5. Loss of BRMS2 decreases CRC cells translation capacity. (A) Nascent protein synthesis was detected by Click-iT HPG after NC-KD or BRMS2-KD HCT116 cells treated with Dox for 3 days. HCT116 cells incubated for 30 min with CHX (50 μg/mL) served as negative controls. (B) The graph showed the quantification of HPG Alexa Fluor 488 fluorescence intensity in (A). (C) Flow cytometry readout for nascent protein synthesis by Click-iT HPG in the different conditions. (D) Quantification of global translation in (C). $^{*}P<0.05$, $^{**}P<0.01$, $^{***}P<0.001$.

been treated as a promising therapeutic target and a large variety of chemotherapeutic drugs have been identified. For example, chemicals blocking rRNA transcription (e.g., actinomycin

D, mitomycin C, mitoxantrone, doxorubicin, cisplatin, oxaliplatin and methotrexate) [27] or pre-rRNA processing (e.g., Camptothecin, flavopiridol, roscovitine, 5-fluorouracil, MG-132, and homoharringtonine) [28] have been used as chemotherapeutic drugs in cancer treatments. In our study, we found knockdown of BRMS2 could impede cell proliferation in CRC cells. Those indicated BRMS2 may function as a potential anti-cancer target. Moreover, no effective inhibitor targeting BRMS2 has been identified. Even though the ribosome biogenesis occurs in both normal and cancer cells, evidences have shown inhibition of ribosome biogenesis selective damaged cancer cells. The higher sensitivity of cancer cells to the inhibitors appears to be the consequence of up-regulate the ribosome biogenesis rate [29-31].

Deletion of one allele of the Rps6 resulted in peri-gastrulation lethality. Cross breeding the Rps6-heterozygous mouse with a p53-null mouse bypassed their lethality until mid-gestation, when the embryos died, showing defective translation of some proteins [32]. This indicates defective translation and p53-dependent checkpoint are two main consequence of impaired ribosome biogenesis. Downregulation of U3 components such as FBL and U3 snoRNAs have been shown to stabilize p53 and activate the IRBC [5, 24]. As a result, we first speculated that BRMS2-depleted HCT116 cells proliferated at a lower rate may result from the same mechanism. However, to our surprise, our results showed that depletion of BRMS2 didn't show accumulation of p53 and induction of IRBC. In addition to the detection of p53 pathway in BRMS2-depleted HCT116 cells, SW620 cells harboring mutated p53 were used to verify the inactivation of IRBC in the present study. Functional p53 is essential in sensing the fidelity of ribosome biogenesis and inducing IRBC. The cell cycle progression would resume if the p53 response could not be induced because of the mutation or deletion even though the ribosome biogenesis was impaired [1]. Our results showed that BRMS2-depleted SW620 cells also proliferated at a lower rate similar to the results in HCT116. This is another proof that BRMS2 depletion may not function through activation of p53.

Although multiple participants in ribosome biogenesis have showed the ability to activate p53 [33], it is generally accepted that RPL5 and RPL11 as well as 5S rRNA play the major roles. This may be that most RPs are rapidly degraded by the proteasome while RPL5 and RPL11 are able to accumulate in a ribosome-free fraction because of their mutual protection from proteasomal degradation [17]. In actinomycin D-induced A549 and U2OS cells, depletion of RPL5 and/or RPL11, significantly abrogated the stabilization of p53 and rescued the arrest of cell cycle [17]. As a result, another approach we took was knocking down BRMS2 in combination with RPL11 at the same time. If IRBC existed in BRMS2-depleted cells, co-silent RPL11 will decrease p53 and recover the low-rate cell proliferation. However, our results was that knockdown of RPL11 could not rescue even aggravate the low-rate cell proliferation in BRMS2-depleted HCT116 cells. This finding was consistent with the phenomenon that loss of RPL11 in primary human lung fibroblasts without undergoing IRBC impedes cell proliferation. They found that the depletion of RPL11 reduced the translation capacity instead of activating p53 pathway. Production of ribosomes controls translation of all proteins in the cell and thus governs cell growth and proliferation [34]. RPL5/RPL11/5S rRNA-Hdm2-dependent IRBC and insufficient translation are two outcomes of impaired ribosome biogenesis [18]. As a result, we detected the translation rate and found it was at a low rate in BRMS2-depleted HCT116 cells. Take together, it can be speculated that BRMS2-depletion-induced low-rate proliferation may result from reduced translation capacity rather than IRBC in the present study. Thus, further investigations are required.

We investigated in several aspects to verify the function of p53 in BRMS2-depleiton-induced growth inhibition and found p53 did not play the key role. However, this was not a meaningless result because these results indicated BRMS2 was much more special than other snoRNP or ribosome components. Depletion of BRMS2 didn't act like the numerous other ribosome processing factors which was capable of inducing IRBC [35-37], nor like RPL11/RPL5 which didn't affect the protein level of p53 [38]. In our study, the protein expression of p53 was slightly depressed and its targets were significantly down-regulated according to BRMS2 depletion. These indicated BRMS2

may play other important roles. For example, could BRMS2 bind to Hdm2 and promote the stabilization of p53 like RPL11? We don't fully understand why BRMS2 is so special and further investigations are needed. Notably, we observed the expression of RPL11 was increased in BRMS2-depleted HCT116 cells. This was consistent with previous study that RPL11 protein was translationally up-regulated upon impairing 40S ribosome biogenesis [39]. Cells could selectively upregulate the translation of RPL11 mRNAs because of its 5' terminal oligopyrimidine tract (5'-TOP mRNAs), despite inhibition of global protein synthesis [38]. As a result, the overexpression of RPL11 indicated that loss of BRMS2 may have the potential ability to induce IRBC but eventually covered by the translation inefficiency of p53 and its targets. Further investigations should be performed to address this hypothesis.

Conclusions

Our study demonstrates that BRMS2 is aberrantly overexpressed in CRC which is correlated with an adverse prognosis. Additionally, silence of BRMS2 impedes CRC cell growth both *in vitro* and *in vivo*. Those indicate BRMS2 could be potential target for CRC therapy. Moreover, the therapeutic effect of targeting BRMS2 is independent of IRBC, but nevertheless companied by translation insufficiency.

Acknowledgements

This work was supported by the National Natural Science Foundation of China (81973358 and 82000481), Natural Science Foundation of Shanghai (20ZR1435000) and the Shanghai Sailing Program (No. 20YF1429400).

Disclosure of conflict of interest

None.

Address correspondence to: Dr. Yili Yang, Suzhou Institute of Systems Medicine, Chinese Academy of Medical Sciences & Peking Union Medical College, Suzhou 215000, China. Tel: +86-0512-62873527; E-mail: yangyl@ism.pumc.edu.cn; Peng Du, Department of Colorectal Surgery, Xin-Hua Hospital, Shanghai Jiaotong University School of Medicine, Shanghai 200092, China. E-mail: dupeng@xinhuamed.com.cn

References

[1] Turi Z, Senkyrikova M, Mistrik M, Bartek J and Moudry P. Perturbation of RNA polymerase I transcription machinery by ablation of HEATR1 triggers the RPL5/RPL11-MDM2-p53 ribosome biogenesis stress checkpoint pathway in human cells. Cell Cycle 2018; 17: 92-101.

[2] Medina-Medina I, Martinez-Sanchez M, Hernandez-Monge J, Fahraeus R, Muller P and Olivares-Illana V. p53 promotes its own polyubiquitination by enhancing the HDM2 and HDMX interaction. Protein Sci 2018; 27: 976-986.

[3] Nicolas E, Parisot P, Pinto-Monteiro C, de Walque R, De Vleeschouwer C and Lafontaine DL. Involvement of human ribosomal proteins in nucleolar structure and p53-dependent nucleolar stress. Nat Commun 2016; 7: 11390.

[4] Gentilella A, Moron-Duran FD, Fuentes P, Zweig-Rocha G, Riano-Canalias F, Pelletier J, Ruiz M, Turon G, Castano J, Tauler A, Bueno C, Menendez P, Kozma SC and Thomas G. Autogenous control of 5'TOP mRNA stability by 40S ribosomes. Mol Cell 2017; 67: 55-70, e54.

[5] Watanabe-Susaki K, Takada H, Enomoto K, Miwata K, Ishimine H, Intoh A, Ohtaka M, Nakanishi M, Sugino H, Asashima M and Kurisaki A. Biosynthesis of ribosomal RNA in nucleoli regulates pluripotency and differentiation ability of pluripotent stem cells. Stem Cells 2014; 32: 3099-3111.

[6] Watkins NJ and Bohnsack MT. The box C/D and H/ACA snoRNPs: key players in the modification, processing and the dynamic folding of ribosomal RNA. Wiley Interdiscip Rev RNA 2012; 3: 397-414.

[7] Rothe B, Manival X, Rolland N, Charron C, Senty-Segault V, Branlant C and Charpentier B. Implication of the box C/D snoRNP assembly factor Rsa1p in U3 snoRNP assembly. Nucleic Acids Res 2017; 45: 7455-7473.

[8] Granneman S, Gallagher JE, Vogelzangs J, Horstman W, van Venrooij WJ, Baserga SJ and Pruijn GJ. The human Imp3 and Imp4 proteins form a ternary complex with hMpp10, which only interacts with the U3 snoRNA in 60-80S ribonucleoprotein complexes. Nucleic Acids Res 2003; 31: 1877-1887.

[9] Bray F, Ferlay J, Soerjomataram I, Siegel RL, Torre LA and Jemal A. Global cancer statistics 2018: GLOBOCAN estimates of incidence and mortality worldwide for 36 cancers in 185 countries. CA Cancer J Clin 2018; 68: 394-424.

[10] Dekker E, Tanis PJ, Vleugels JLA, Kasi PM and Wallace MB. Colorectal cancer. Lancet 2019; 394: 1467-1480.

[11] Xu W, Sheng Y, Guo Y, Huang Z, Huang Y, Wen D, Liu CY, Cui L, Yang Y and Du P. Increased IGF2BP3 expression promotes the aggressive phenotypes of colorectal cancer cells in vitro and vivo. J Cell Physiol 2019; 234: 18466-18479.
[12] Geng X, Liu Y, Dreyer T, Bronger H, Drecoll E, Magdolen V and Dorn J. Elevated tumor tissue protein expression levels of kallikrein-related peptidases KLK10 and KLK11 are associated with a better prognosis in advanced high-grade serous ovarian cancer patients. Am J Cancer Res 2018; 8: 1856-1864.
[13] Bajikar SS, Wang CC, Borten MA, Pereira EJ, Atkins KA and Janes KA. Tumor-suppressor inactivation of GDF11 occurs by precursor sequestration in triple-negative breast cancer. Dev Cell 2017; 43: 418-435, e413.
[14] Juli G, Gismondi A, Monteleone V, Caldarola S, Iadevaia V, Aspesi A, Dianzani I, Proud CG and Loreni F. Depletion of ribosomal protein S19 causes a reduction of rRNA synthesis. Sci Rep 2016; 6: 35026.
[15] Wu Z, Mata M and Fink DJ. Prolonged regulatable expression of EPO from an HSV vector using the LAP2 promoter element. Gene Ther 2012; 19: 1107-1113.
[16] Liu J, Xu Y, Stoleru D and Salic A. Imaging protein synthesis in cells and tissues with an alkyne analog of puromycin. Proc Natl Acad Sci U S A 2012; 109: 413-418.
[17] Bursac S, Brdovcak MC, Pfannkuchen M, Orsolic I, Golomb L, Zhu Y, Katz C, Daftuar L, Grabusic K, Vukelic I, Filic V, Oren M, Prives C and Volarevic S. Mutual protection of ribosomal proteins L5 and L11 from degradation is essential for p53 activation upon ribosomal biogenesis stress. Proc Natl Acad Sci U S A 2012; 109: 20467-20472.
[18] Teng T, Mercer CA, Hexley P, Thomas G and Fumagalli S. Loss of tumor suppressor RPL5/RPL11 does not induce cell cycle arrest but impedes proliferation due to reduced ribosome content and translation capacity. Mol Cell Biol 2013; 33: 4660-4671.
[19] Gerczei T and Correll CC. Imp3p and Imp4p mediate formation of essential U3-precursor rRNA (pre-rRNA) duplexes, possibly to recruit the small subunit processome to the pre-rRNA. Proc Natl Acad Sci U S A 2004; 101: 15301-15306.
[20] Grandi P, Rybin V, Bassler J, Petfalski E, Strauss D, Marzioch M, Schafer T, Kuster B, Tschochner H, Tollervey D, Gavin AC and Hurt E. 90S pre-ribosomes include the 35S pre-rRNA, the U3 snoRNP, and 40S subunit processing factors but predominantly lack 60S synthesis factors. Mol Cell 2002; 10: 105-115.
[21] Thomson E, Ferreira-Cerca S and Hurt E. Eukaryotic ribosome biogenesis at a glance. J Cell Sci 2013; 126: 4815-4821.
[22] White RJ. RNA polymerases I and III, growth control and cancer. Nat Rev Mol Cell Biol 2005; 6: 69-78.
[23] Grummt I. Wisely chosen paths--regulation of rRNA synthesis: delivered on 30 June 2010 at the 35th FEBS Congress in Gothenburg, Sweden. FEBS J 2010; 277: 4626-4639.
[24] Langhendries JL, Nicolas E, Doumont G, Goldman S and Lafontaine DL. The human box C/D snoRNAs U3 and U8 are required for pre-rRNA processing and tumorigenesis. Oncotarget 2016; 7: 59519-59534.
[25] Su H, Xu T, Ganapathy S, Shadfan M, Long M, Huang TH, Thompson I and Yuan ZM. Elevated snoRNA biogenesis is essential in breast cancer. Oncogene 2014; 33: 1348-1358.
[26] Ruggero D and Pandolfi PP. Does the ribosome translate cancer? Nat Rev Cancer 2003; 3: 179-192.
[27] Bruno PM, Liu Y, Park GY, Murai J, Koch CE, Eisen TJ, Pritchard JR, Pommier Y, Lippard SJ and Hemann MT. A subset of platinum-containing chemotherapeutic agents kills cells by inducing ribosome biogenesis stress. Nat Med 2017; 23: 461-471.
[28] Burger K, Muhl B, Harasim T, Rohrmoser M, Malamoussi A, Orban M, Kellner M, Gruber-Eber A, Kremmer E, Holzel M and Eick D. Chemotherapeutic drugs inhibit ribosome biogenesis at various levels. J Biol Chem 2010; 285: 12416-12425.
[29] Brighenti E, Trere D and Derenzini M. Targeted cancer therapy with ribosome biogenesis inhibitors: a real possibility? Oncotarget 2015; 6: 38617-38627.
[30] Quin JE, Devlin JR, Cameron D, Hannan KM, Pearson RB and Hannan RD. Targeting the nucleolus for cancer intervention. Biochim Biophys Acta 2014; 1842: 802-816.
[31] Hein N, Hannan KM, George AJ, Sanij E and Hannan RD. The nucleolus: an emerging target for cancer therapy. Trends Mol Med 2013; 19: 643-654.
[32] Panic L, Tamarut S, Sticker-Jantscheff M, Barkic M, Solter D, Uzelac M, Grabusic K and Volarevic S. Ribosomal protein S6 gene haploinsufficiency is associated with activation of a p53-dependent checkpoint during gastrulation. Mol Cell Biol 2006; 26: 8880-8891.
[33] Golomb L, Volarevic S and Oren M. p53 and ribosome biogenesis stress: the essentials. FEBS Lett 2014; 588: 2571-2579.
[34] Rudra D and Warner JR. What better measure than ribosome synthesis? Genes Dev 2004; 18: 2431-2436.

[35] Skarie JM and Link BA. The primary open-angle glaucoma gene WDR36 functions in ribosomal RNA processing and interacts with the p53 stress-response pathway. Hum Mol Genet 2008; 17: 2474-2485.
[36] McMahon M, Ayllon V, Panov KI and O'Connor R. Ribosomal 18 S RNA processing by the IGF-I-responsive WDR3 protein is integrated with p53 function in cancer cell proliferation. J Biol Chem 2010; 285: 18309-18318.
[37] Yu W, Qiu Z, Gao N, Wang L, Cui H, Qian Y, Jiang L, Luo J, Yi Z, Lu H, Li D and Liu M. PAK1IP1, a ribosomal stress-induced nucleolar protein, regulates cell proliferation via the p53-MDM2 loop. Nucleic Acids Res 2011; 39: 2234-2248.
[38] Fumagalli S, Di Cara A, Neb-Gulati A, Natt F, Schwemberger S, Hall J, Babcock GF, Bernardi R, Pandolfi PP and Thomas G. Absence of nucleolar disruption after impairment of 40S ribosome biogenesis reveals an rpL11-translation-dependent mechanism of p53 induction. Nat Cell Biol 2009; 11: 501-508.
[39] Fumagalli S, Ivanenkov VV, Teng T and Thomas G. Suprainduction of p53 by disruption of 40S and 60S ribosome biogenesis leads to the activation of a novel G2/M checkpoint. Genes Dev 2012; 26: 1028-1040.

Table S1. The primers and shRNA sequences used in this study

Name	Sequences
IMP3	F: CTGACGTGGTTACCGACCC
	R: TCGCGCTCCTCATTGTACTC
RPL11	F: TTCGCATCCGCAAACTCTGT
	R: TTCTCCGGATGCCAAAGGAT
Pre-47s	F: GCTGACACGCTGTCCTCTG
	R: ACGCGCGAGAGAACAGCAG
p53	F: TGTGACTTGCACGTACTCCC
	ACCATCGCTATCTGAGCAGC
p21	F: TGTGGACCTGTCACTGTCTT
	R: GAGTGGTAGAAATCTGTCATGCT
GADD45G	F: GACACAGTTCCGGAAAGCAC
	R: TTGGCTGACTCGTAGACGC
GAPDH	F: ACCCAGAAGACTGTGGATGG
	R: CAGTGAGCTTCCCGTTCAG
shNC	CCGGTTCTCCGAACGTGTCACGTCTCGAGACGTGACACGTTCGGAGAATTTTTG
	AATTCAAAAATTCTCCGAACGTGTCACGTCTCGAGACGTGACACGTTCGGAGAA
shBRMS2#	CCGGCAGACGGTCGTAGGTTCTTAACTCGAGTTAAGAACCTACGACCGTCTGTTTTTG
	AATTCAAAAACAGACGGTCGTAGGTTCTTAACTCGAGTTAAGAACCTACGACCGTCTG
shRPL11#	CCGGGCGGGAGTATGAGTTAAGAAACTCGAGTTTCTTAACTCATACTCCCGCTTTTTG
	AATTCAAAAAGCGGGAGTATGAGTTAAGAAACTCGAGTTTCTTAACTCATACTCCCGC

#Three gene-specific shRNAs were designed and the highest efficiency one was presented here and used in further investigation.